Journal of Neurochemistry

JOURNAL OF NEUROCHEMISTRY | 2015 | 132 | 169–182 doi: 10.1111/jnc.12967

ORIGINAL ARTICLE

P301L tau expression affects glutamate release and clearance in the hippocampal trisynaptic pathway

Holly C. Hunsberger,* Carolyn C. Rudy,* Seth R. Batten,† Greg A. Gerhardt† and Miranda N. Reed*,‡,§

*Behavioral Neuroscience, Department of Psychology, West Virginia University, Morgantown, West Virginia, USA

†Center for Microelectrode Technology (CenMeT), Department of Anatomy and Neurobiology, University of Kentucky Health Sciences Center, Lexington, Kentucky

‡Center for Neuroscience, West Virginia University, Morgantown, West Virginia, USA

§Center for Basic and Translational Stroke Research, West Virginia University, Morgantown, West Virginia, USA

Abstract

Individuals at risk of developing Alzheimer's disease (AD) often exhibit hippocampal hyperexcitability. A growing body of evidence suggests that perturbations in the glutamatergic tripartite synapse may underlie this hyperexcitability. Here, we used a tau mouse model of AD (rTg(TauP301L) 4510) to examine the effects of tau pathology on hippocampal glutamate regulation. We found a 40% increase in hippocampal vesicular glutamate transporter, which packages glutamate into vesicles, and has previously been shown to influence glutamate release, and a 40% decrease in hippocampal glutamate transporter 1, the major glutamate transporter responsible for removing glutamate from the extracellular space. To determine whether these alterations affected glutamate regulation *in vivo*, we measured tonic glutamate levels, potassium-evoked glutamate release, and glutamate uptake/clearance in the dentate gyrus, cornu ammonis 3(CA3), and cornu ammonis 1(CA1) regions of the hippocampus. P301L tau expression resulted in a 4- and 7-fold increase in potassium-evoked glutamate release in the dentate gyrus and CA3, respectively, and significantly decreased glutamate clearance in all three regions. Both release and clearance correlated with memory performance in the hippocampal-dependent Barnes maze task. Alterations in mice expressing P301L were observed at a time when tau pathology was subtle and before readily detectable neuron loss. These data suggest novel mechanisms by which tau may mediate hyperexcitability.

Keywords: Alzheimer, glutamate clearance, hippocampus, *in vivo* electrochemistry, synaptic release, tau.

J. Neurochem. (2015) **132**, 169–182.

Alzheimer's disease (AD) affects approximately 5.4 million Americans and is often characterized by progressive memory loss, decline in cognitive skills, and adverse behavioral changes (Thies and Bleiler 2013). Biologically, AD is characterized by an abundance of extracellular amyloid plaques, comprised of aggregates of beta-amyloid (Aβ), and intracellular neurofibrillary tangles (NFTs) containing hyperphosphorylated tau protein (Serrano-Pozo *et al.* 2011). Another major feature of AD is neurodegeneration that may relate to neural network dysfunction (Buckner *et al.* 2005; Palop *et al.* 2006; Seeley *et al.* 2009). Recent work suggests that tau-related pathology begins in vulnerable regions of the brain, including the entorhinal cortex and hippocampus, part of the brain's memory network, before spreading to other cells along the same neural network (de Calignon *et al.* 2012; Liu *et al.* 2012; Nath *et al.* 2012).

Received August 29, 2014; revised manuscript received September 25, 2014; accepted October 2, 2014.

Correspondence and present address: Miranda N. Reed, 53 Campus Drive, Morgantown, WV 26506, USA. E-mail: miranda.reed@mail.wvu.edu

Abbreviations used: AD, Alzheimer's disease; Aβ, amyloid-beta; BM, Barnes maze; CA1, cornu ammonis 1; CA3, cornu ammonis 3; DG, dentate gyrus; EC, extracellular; GLT-1, glutamate transporter 1; GluOx, glutamate oxidase; H&E, hematoxylin and eosin; LTP, long-term potentiation; MEA, microelectrode array; mPD, m-phenylenediamine; NFTs, neurofibrillary tangles; TRE, tetracycline response element; tTA, tetracycline-controlled transcriptional activation; vGLUT1, vesicular glutamate transporter 1.

Effective regulation of activity in these neural networks is essential because both increases and decreases in stimulation can impair neuronal function and survival, while neural network dysfunction could contribute directly to the neurodegenerative process (Palop *et al.* 2006). An early feature in aging, before AD pathology, is the hyperactivity of the memory network, particularly hippocampal regions. In studies using functional magnetic resonance imaging (fMRI), elevated hippocampal activation is observed in individuals at risk for AD, including cognitively normal carriers of the apolipoprotein E4 (ApoE4) allele, a known genetic risk factor for AD (Trivedi *et al.* 2008; Filippini *et al.* 2009; Dennis *et al.* 2010), pre-symptomatic carriers of genetic mutations in familial AD (Quiroz *et al.* 2010), and patients with mild cognitive impairment (MCI) (Dickerson *et al.* 2005; Hamalainen *et al.* 2007). Longitudinal fMRI assessments of ApoE4 allele carriers indicate that hippocampal over-activation correlates with declines in memory (Bookheimer *et al.* 2000). Furthermore, patients with MCI exhibit greater hippocampal activation during memory encoding (Dickerson *et al.* 2004, 2005; Celone *et al.* 2006; Sperling 2007), and increased activation in MCI is predictive of the degree and rate of cognitive decline and conversion to AD (Miller *et al.* 2008).

Hippocampal hyperactivity was once believed to serve as a compensatory function for deteriorating circuitry by recruiting extra neural resources (i.e., greater cognitive effort to achieve comparable performance) (Grady *et al.* 2003; Ward and Frackowiak 2003; Bondi *et al.* 2005). However, more recent studies show that excess activation may contribute directly to memory impairment and AD-related pathology and could represent a therapeutic target. Circumstantial human evidence supports this view. For example, seizures and epileptiform activity are associated with an early age at onset of cognitive decline and precede or coincide with diagnosis of MCI or AD (Vossel *et al.* 2013). However, the relation between hyperactivity and memory impairments may be more than correlational (Sanchez *et al.* 2002; Koh *et al.* 2010; Bakker *et al.* 2012). Treatments targeting excess hippocampal activation dose dependently improved memory performance in memory-impaired aged rats; these same doses had no effect in young rats without memory impairments, suggesting that dampening of hippocampal hyperactivity, not merely a global cognitive enhancement, was responsible for the memory improvement in aged rats (Koh *et al.* 2010). Furthermore, a reduction in aberrant neural network activity reversed the synaptic and cognitive deficits observed in a mouse model of AD (Sanchez *et al.* 2012). Evidence for the adverse consequences of hyperexcitability has also been shown in humans; reducing hippocampal activation in an amnestic MCI group improved memory performance (Bakker *et al.* 2012). Together, these studies suggest that increased hippocampal activation is not merely a compensatory response but a dysfunctional condition, and a condition that may be permissive for the development of AD.

Recent work suggests that tau may mediate hyperexcitability. Genetic removal of tau decreases seizure activity in an Aβ mouse model of AD (Roberson *et al.* 2011). Furthermore, in this same mouse model, reducing endogenous tau ameliorated excitotoxicity and rescued cognitive dysfunction, without altering Aβ levels (Roberson *et al.* 2007), suggesting tau, not Aβ, was mediating excitotoxicity. Deletion of tau in mouse and drosophila models of epilepsy also reduces hyperexcitability, as well as seizure frequency and duration (Daniels *et al.* 2011). The exact mechanism for these changes remains to be determined, but recent work suggests that tau may alter glutamate neurotransmission (Roberson *et al.* 2007, 2011; Timmer *et al.* 2014).

To examine the role of tau in glutamate dysregulation, we used the most commonly used tau mouse model of AD, the rTg(TauP301L)4510 (hereafter called TauP301L) mouse model. These mice exhibit age-dependent cognitive decline, neurofibrillary tangle deposition, and neuron loss (Ramsden *et al.* 2005; SantaCruz *et al.* 2005). However, previous work suggests that TauP301L mice exhibit electrophysiological hyperexcitability prior to tangle deposition or neuronal death (Crimins *et al.* 2012). Here, we sought to examine the effects of P301L expression on glutamate regulation at an age when subtle memory deficits and tau pathology are detectable but before neuron loss or tangle deposition occurs. This allowed us to dissociate the memory loss and any glutamate alterations resulting from P301L human tau expression with that associated with neuronal loss and to potentially provide an explanation for the electrophysiological hyperexcitability observed in this model.

Prior to examination of glutamate regulation, mice were memory tested using the hippocampal-dependent Barnes maze (BM) task to ensure the presence of subtle memory impairments at the age tested. *In vivo* glutamate regulation was measured in the dentate gyrus (DG), cornu ammonis (CA)3, and CA1 subregions of the hippocampus, areas rich in glutamate receptors (Pettit and Augustine 2000; Nimchinsky *et al.* 2004), using ceramic-based microelectrode arrays coupled with amperometry. This approach allowed us to selectively measure extracellular glutamate at 10 Hz and compare tonic glutamate levels, potassium-evoked (KCl) glutamate release, and glutamate uptake/clearance among the groups (Burmeister *et al.* 2000; Burmeister and Gerhardt 2001). Another benefit of microelectrode arrays over other *ex vivo* methods is the ability to study brain regions *in vivo* without disrupting their extrinsic and intrinsic connections, a particularly important consideration when examining the complex connections of the trisynaptic loop of the hippocampus. Because examination of memory and glutamate regulation was done within the same animal, we were able to relate changes in glutamatergic signaling with behavioral

changes. This study suggests that targeting excess hippocampal activity may have therapeutic potential for the treatment of AD.

Methods

Subjects

Creation of TauP301L mice has been described (Ramsden *et al.* 2005; SantaCruz *et al.* 2005; Hoover *et al.* 2010). Briefly, regulatable transgenic mice expressing human four-repeat tau lacking the N-terminal sequences (4R0N) with a P301L mutation were created by crossing a responder and activator line. Responder mice (FVB/N background strain), heterozygous for the tetracycline response element (TRE)-TauP301L transgene, were bred with heterozygous activator mice (129S6 background strain) that express the tet-off tetracycline transactivator (tTA) reading frame placed downstream of Ca^{2+}/calmodulin kinase II promoter elements (SantaCruz *et al.* 2005). The four genotypes of animals generated are described by the following nomenclature, TauP301L/CKtTA, and include what we refer to as TauP301L mice (+/+) and Controls (−/+, +/−, −/−). In this study, we used the −/+ control because no behavioral differences among the three control groups have been reported, and human tau is not expressed in any of the controls (Ramsden *et al.* 2005; SantaCruz *et al.* 2005; Hoover *et al.* 2010), yet the −/+ allowed us to control for the expression of tTA (Mayford *et al.* 1996).

To control for the over-expression of human tau, we also examined the rTg(TauWT) 21221 mouse model (hereafter called TauWT). TauWT mice express wild-type 4R0N human tau at concentrations equivalent to P301L human tau in TauP301L mice, but without the P301L mutation, and show no NFTs, progressive memory decline nor neurodegeneration (Hoover *et al.* 2010). TauWT were generated in the same way as TauP301L mice.

The Ca^{2+}/calmodulin kinase II promoter was used to restrict TauP301L protein expression to the forebrain (SantaCruz *et al.* 2005), which contains the brain regions most severely affected in AD (Auld *et al.* 2002), while the tet-off system allowed for regulatable expression of the tau protein. In the tet-off system, the tTA protein binds to TRE in the absence of doxycycline, allowing transcription and protein expression to occur (Liu *et al.* 2008), whereas in the presence of doxycycline, the tTA protein cannot bind to TRE, allowing tau expression to be suppressed. Previously published work suggests that developmental P301L tau expression produces alterations not observed following adult-onset tau expression (Caouette *et al.* 2013), possibly because of the important role of tau in brain development (Wang and Liu 2008). To avoid mutant tau expression during the perinatal and early postnatal stages, thereby preventing developmental alterations unrelated to AD, tau was suppressed during brain development (Hunsberger *et al.* 2014). To suppress tau, 40 ppm doxycycline hyclate was administered via water bottles to breeder dams for 3 weeks prior to mating and to all experimental female mice from birth until 2 months of age (Hölscher 1999). Behavioral testing began at 5 months of age, after 3 months of tau expression, and was followed by glutamate function testing. All experimental procedures were conducted in accordance with the standards of International Animal Care and Use Committee, and the West Virginia University Animal Care and Use Committee approved all experimental procedures.

Barnes maze

The BM consists of a circular white platform (122 cm), 108 cm above the ground, with 40 holes (5 cm), one with a hidden escape box. Training was performed as previously described with slight modification (McLay *et al.* 1998; McAfoose *et al.* 2009). For the 2 days preceding acquisition trials, the mice were habituated to the maze. There were no extra-maze cues during habituation training. During the first day of habituation, the mice were placed under a clear beaker and allowed to enter the escape box for 5 min. The next day, the mouse was gently guided to the escape box and allowed to remain in the escape box for 2 min. Each mouse completed two trials each day with approximately 20–25 min between trials.

For acquisition training on days 3–7, extra-maze cues were placed around the room, and weak aversive stimulation was applied to increase the motivation to escape from the circular platform; aversive stimulation included the illumination of overhead lights and the use of four fans evenly placed around the maze. At the start of the trial, the mouse was placed under a plastic beaker in the center of the platform. After 10 s, the beaker was raised, and the mouse was free to explore. The trials ended 30 s after the mouse entered the escape box. If the mouse did not enter the escape box during the 3-min trial, the experimenter gently guided the mouse into the escape box and covered the hole for 30 s. Mice received three trials per day with 20–25 min between trials. The maze was cleaned with 70% ethanol, rotated clockwise after every trial to avoid intramaze odor or visual cues, although the escape box remained in the same place relative to extra-maze cues. Latency to reach the escape box and number of errors before reaching the escape box were recorded.

The first of two probe trials, in which the escape box was removed, took place 24 h after the last acquisition trial. The second probe trial took place 1 week following the first probe trial. Probe trials lasted 90 s. Latency to reach the target hole and the number of errors made were recorded. Because of the long duration of the probe trial and to further evaluate search strategy, as previously described (e.g., Devan *et al.* 2003), the probe trial was divided into three 30-s epochs, and errors evaluated in each epoch separately.

Enzyme-based microelectrode arrays

Ceramic-based microelectrode arrays (MEAs) were used to examine glutamate regulation and were purchased from Quanteon, L.L.C. (Nicholasville, KY, USA). The array consisted of a ceramic-based multisite microelectrode with four platinum recording sites (Burmeister and Gerhardt 2001). These sites were arranged in dual pairs to allow interfering agents to be detected and removed from the analyte signal (Burmeister and Gerhardt 2001). Coating of the microelectrodes has been described previously (Hinzman *et al.* 2010). Briefly, the recording sites were covered with glutamate oxidase to oxidize glutamate to alpha-ketoglutarate and hydrogen peroxide (H_2O_2), the reporter molecule (Burmeister and Gerhardt 2001). An inactive protein matrix covered the other pair of recording sites (sentinel sites). Small molecules, like H_2O_2, can diffuse through the m-phenylenediamine exclusion layer, but not larger molecules such as ascorbic acid or monoamines. The background current from the sentinel sites was then subtracted from the recording sites to produce a selective measure of extracellular glutamate. A reference electrode Ag/AgCl was implanted into a remote site from the recording area (Burmeister and Gerhardt 2001).

Calibration

Calibrations were conducted on the MEAs prior to their use to ensure sensitivity and selectivity and to create a standard curve for the conversion of current to glutamate concentration. Using the FAST-16 mkII system (Quanteon LLC, Nicholasville, KY, USA), a constant potential of + 0.7 V versus an Ag/AgCl reference was applied to the MEA to oxidize the reporter molecule. The resulting current was amplified, digitized, and filtered by the FAST 16 mkII system. The MEA tip was submerged in 40 mL of a 0.05 M phosphate-buffered saline maintained at 37°C. A standard curve was determined by adding successive aliquots of 20 μL glutamate to achieve concentrations of 20, 40, and 60 μM. The increase in current (nA) produced by oxidation was used to calculate the calibration slope to a known concentration of glutamate (Burmeister *et al.* 2002). To determine the selectivity for glutamate, ascorbic acid (250 μM) and dopamine (2 μM) were added to the solution (Hinzman *et al.* 2012). To determine the limit of detection (LOD), the smallest concentration of glutamate that can be measured by the device, the slope of the standard curve was used, as well as the noise or relative standard deviation of the baseline signal (Hinzman *et al.* 2012).

MEA/micropipette assembly

For intracranial drug deliveries, a glass micropipette with an inner diameter tip of 10–15 μm (Quanteon) was attached to the MEA. The micropipette was centered between the dorsal and ventral platinum recording pairs and positioned 80–100 μm away from the MEA surface. Location of the micropipette to the MEA was verified post surgery to ensure that the pipette did not move. The micropipette was back-filled with sterile-filtered isotonic KCl solution (70 mM KCl, 79 mM NaCl, 2.5 mM $CaCl_2$, pH 7.4) or glutamate solution (200 μM glutamate, pH 7.4). The micropipette was attached to a Picospritzer III (Parker-Hannifin, Cleveland, OH, USA) and set to consistently deliver volumes of 50–100 nL. Pressure was applied from 2 to 20 psi (0.138–1.38 bar; 13.8–137.8 kPa) for 0.30–2.5 s. Volume displacement was monitored with the use of a stereomicroscope fitted with a reticule (Friedemann and Gerhardt 1992).

In vivo anesthetized recordings

Mice were anesthetized with isoflurane (1–4% inhalation; continuous) and placed into a stereotaxic apparatus (David Kopf Instruments, Tujunga, CA, USA). Isoflurane was used because other anesthetics have been shown to have great effects on resting glutamate levels (Mattinson *et al.* 2011). Although initial reports suggested that isoflurane increases tau phosphorylation (Planel *et al.* 2004), more recent reports suggest that when anesthesia-induced hypothermia is controlled for, isoflurane does not increase tau phosphorylation (Tan *et al.* 2010). To ensure mice did not become hypothermic while under anesthesia, body temperature was continuously measured using a rectal probe and maintained at 37°C with a water pad connected to a recirculating water bath (Gaymar Industries Inc., Orchard Park, NY, USA).

A craniotomy was performed to allow access to the hippocampus for MEA recordings. The Ag/AgCl wire reference electrode was placed under the skin with a saline-soaked gauze pad in the hemisphere opposite from the recording sites. The MEA/micropipette array was placed into the DG, CA3, and CA1 of the hippocampus, subregions rich in glutamate receptors (Pettit and Augustine 2000; Nimchinsky *et al.* 2004). Stereotaxic coordinates for the different subregions of the hippocampus were calculated using the mouse brain atlas (Paxinos & Franklin 2012) [DG (AP: −2.3 mm, ML: +/−1.5 mm, DV: 2.1 mm), CA3 (AP: −2.3 mm, ML: +/−2.7 mm, DV: 2.25 mm), CA1 (AP: −2.3 mm, ML: +/−1.7 mm, DV: 1.4 mm)] and confirmed post mortem. All MEA recordings were performed at 10 Hz using constant potential amperometry recordings with the FAST-16. After the MEA reached a stable baseline (10–20 min), tonic glutamate levels (μM) were calculated averaging extracellular glutamate levels over 10 s prior to any application of solutions. In all three subregions of one hemisphere, evoked release (i.e., amplitude) was measured by local application of KCl delivered every 2–3 min. KCl-evoked release of glutamate is highly reproducible and indicative of the intact glutamate neuronal system that is detected by the MEAs (Day *et al.* 2006). After 10 reproducible signals, the results were averaged for each group and the average amplitude compared (Nickell *et al.* 2007; Hinzman *et al.* 2010, 2012). KCl-evoked release of glutamate was measured to determine the "capacity" of the nerve terminals to release glutamate (Hinzman *et al.* 2010).

To examine the glutamate clearance/uptake, exogenous glutamate was applied in the opposite hemisphere. After the MEA reached a stable baseline (10–20 min), varying volumes of 200 μM sterile-filtered glutamate solution were applied into the extracellular space every 2–3 min. Glutamate signals with amplitudes of 40 μM or below were analyzed as this was the physiological range of KCl-evoked glutamate release observed in this study and previous studies (Hinzman *et al.* 2010). The net area under the curve (AUC) was used to estimate glutamate clearance. The hemispheres used for KCl and glutamate application were counterbalanced, as was the order of subregions within a hemisphere. After recording from all locations, an MEA with an attached micropipette was used to locally apply Fluoro-Ruby (Millipore, Bedford, MA, USA) or fast green (Sigma, St Louis, MO, USA), which was used to confirm MEA placement following brain sectioning (Fig. 1). Prior studies have shown that the MEAs produce minimal effects both acutely and chronically (Hascup *et al.* 2009). All behaviorally tested mice underwent glutamate examination. However, data from some hippocampal regions were excluded for reasons including death during surgery, poor placement of the MEA, or in the case of the glutamate uptake studies, amplitudes greater than 40 μM. For each measure, the number of mice per group is provided in the corresponding figure caption.

Immunoblotting

To ensure application of KCl or exogenous glutamate did not influence protein expression, hippocampal tissues from mice not used for glutamate testing were used to assess vesicular glutamate transporter 1 (vGLUT1) and GLT-1 expression. Hippocampal tissue was prepared for immunoblotting using 500-μL radioimmunoprecipitation lysis buffer (50 mM Tris-HCl pH 7.4, 150 mM NaCl, 0.5% Triton X-100, 1 mM EDTA, 3% sodium dodecyl sulfate, 1% Na deoxycholate) with Roche protease inhibitor tablets (EDTA-free Easy pack tablets, Phosphostop Easy pack tablets) added the day of extraction. Protein concentrations were determined with a bicinchoninic acid protein assay using bovine serum albumin as a standard.

Hippocampal tissue samples were thawed and 10-μg aliquots were mixed with loading buffer (450 mM Tris HCL, pH 8, 8%

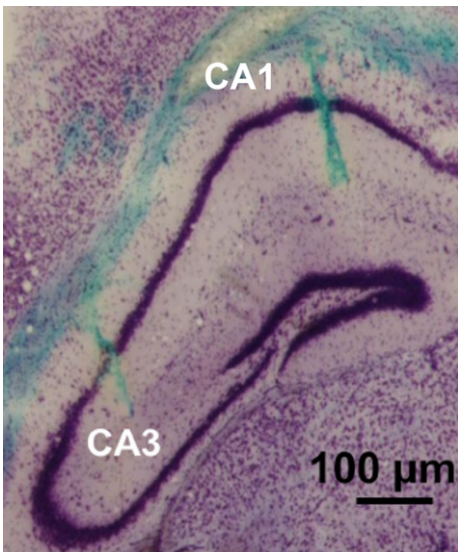

Fig. 1 Cresyl violet-stained 20-µm section of hippocampus shows location of microelectrode array (MEA) tracks in cornu ammonis (CA)3 and CA1.

sodium dodecyl sulfate, 24% glycerol, 5% mercaptoethanol, 0.1% bromophenol blue, 0.1% phenol red). Before loading, samples were either heated to 70°C (vGLUT1 and synaptophysin) or 95°C (GLT-1 and actin I-19) for 5 min and then separated on 10% criterion gels (#345-0009; Bio-Rad Laboratories, Hercules, CA, USA), and transferred onto 0.45 µm polyvinylidene difluoride membranes (Millipore). Membrane blots were blocked for 1 h at ~23 °C in 5% bovine serum albumin in 0.1% Tween 20/Tris-buffered saline (198.5 mM NaCl, 9.98 mM Trizma base, pH 7.4) (vGLUT1, synaptophysin, and actin) or 5% milk in Tween 20/Tris-buffered saline (Non-fat dry milk, Cell Signaling Technology, Beverly, MA, USA) (GLT-1). After blocking, membranes were incubated with an antibody directed against the protein of interest (vGLUT1, 1 : 6000; GLT-1, 1 : 10 000, synaptophysin, 1 : 200; actin I-19, 1 : 500) overnight at 4°C. The next day, membranes were incubated with Streptactin-horseradish peroxidase (Bio-Rad Laboratories) and the appropriate biotinylated or horseradish peroxidase-conjugated secondary antibody for 1.5 h at ~23 °C. Blots were then sprayed 5–10 times evenly with Rapidstep enhanced chemiluminescence (Calbiochem, San Diego, CA, USA), incubated for 5 min, and visualized using Fluorchem E imager (Proteinsimple, Santa Clara, CA, USA). Membranes used to detect vGLUT1 or GLT-1 signals were first probed with vGLUT1 or GLT-1 antibody, then stripped for 1 h with Restore PLUS western blot stripping buffer (Pierce, Rockford, IL, USA), and re-probed with synaptophysin or actin antibody, respectively. vGLUT and GLT-1 bands were normalized to synaptophysin or actin, respectively. Band density was measured using AlphaView software (Proteinsimple, Santa Clara, CA, USA).

Immunohistochemistry

Immunohistochemical detection of total and phosphorylated tau species in transgenic and control mice was performed as described previously (Ramsden *et al.* 2005; Hoover *et al.* 2010). To ensure the application of KCl or exogenous glutamate did not influence tau phosphorylation, tissue from mice not used for glutamate testing was utilized for IHC. Briefly, hemibrains were immersion fixed in 10% formalin for 24–48 h and embedded in paraffin. Serial sections were cut at 5 µm using a microtome, mounted onto CapGap slides (Thermo-Fisher, Waltham, MA, USA), and rehydrated according to the standard protocols. Mounted slides were pre-treated with a citrate buffer (pH 6.0) in a Black & Decker (Owings, MD, USA) steamer for 30 min, with a 10-min cool down. Standard 2-day immunostaining procedures using peroxidase-labeled streptavidin and diaminobenzidine chromagen on an automated TechMate 500 capillary gap immunostainer (Ventana Medical Systems, Tucson, AZ, USA) were used with antibodies directed against (Table 1). Hematoxylin counter-staining was used to provide cytological detail. Hematoxylin and eosin and modified Bielschowsky silver staining to detect NFTs were performed using the standard histological techniques. Photomicrographs of hippocampal and cortical neurons were captured at three different magnifications (×5, ×10, and ×40) with a Zeiss Axioskop microscope coupled to a CCD camera and processed and assembled in Adobe Photoshop (San Jose, CA, USA). No positive labeling was observed for pathological tau epitopes in non-transgenic mice.

Data analysis

All statistical analyses were performed using JMP (SAS, Cary, NC, USA). Statistical analysis consisted of ANOVA and repeated-measures ANOVA (RMANOVA), followed by Tukey *post hoc* comparisons. For the RMANOVA of behavioral data, transgene status served as the between-subject variable, and session served as the within-subject variable. Amperometric data were analyzed using a custom Microsoft excel software program (MatLab, Natick, MA, USA). To determine the

Table 1 Tau antibodies

Antibody	Species	Specificity	Use	Dilution	Source
MC-1	Mouse	Tau; conformational epitope, 7–9 and 326–330 aa	Conformation specific; early pathological change in AD	1 : 8000	P. Davies, The Feinstein Institute for Medical Research, Manhasset, NY, USA
CP-13	Mouse	Tau; $pSer^{202}$	Phosphorylation specific; early pathological change in AD	1 : 2000	P. Davies
AT-8	Mouse	Tau; $pSer^{202}/pThr^{205}$	Pre-tangles; mid-stage	1 : 4000	Innogenetics, Technologiepark, Gent, Belgium
PG-5	Mouse	Tau; $pSer^{409}$	Pre-tangles; mid-stage	1 : 200	P. Davies
NeuN	Mouse	NeuN	Neuronal marker	1 : 4000	Chemicon, Billerica, MA, USA

concentrations of glutamate in the hippocampus, the background current from the sentinel sites was subtracted from the signal obtained from the glutamate oxidase recording sites. The resting current (pA) was divided by the slope (μM/pA) obtained during calibration and reported as a concentration of glutamate. Using Pearson r correlations, KCl-evoked glutamate release (amplitude) and glutamate clearance (net AUC) in the DG, CA3, and CA1 were correlated separately with performance in the BM (errors). Correlations were run only for those mice in which data for both behavior and glutamate were analyzed.

Results

Alterations in hippocampal vGLUT1 and GLT-1 expression in TauP301L mice

Hippocampal vGLUT1 expression was significantly increased in TauP301L mice [$F(2, 14) = 8.65, p = 0.004$]. To determine if there was a widespread increase in pre-synaptic terminals and to serve as a loading control, synaptophysin immunoblotting was performed. No statistically significant difference in synaptophysin expression was observed among the groups [$F(2, 14) = 1.94$, $p = 0.18$]. The ratio of vGLUT1 to synaptophysin was also significantly increased in TauP301L mice [$F(2, 14) = 8.08, p = 0.005$] (Fig. 2a).

Comparison of hippocampal GLT-1 expression revealed a significant decrease in TauP301L mice [$F(2, 13) = 4.94$, $p = 0.03$], but no differences among the groups for the loading control, β-actin [$F(2, 13) = 0.56$, $p = 0.59$]. The ratio of GLT-1 to β-actin was also significantly lower in the hippocampus of TauP301L mice [$F(2, 13) = 6.59, p = 0.01$] (Fig. 2b).

Spatial learning and memory deficits in TauP301L mice

During acquisition, latency did not differ among the groups [Tg main effect: $F(2, 25) = 1.45$, $p = 0.25$; Tg × Day interaction: $F(8, 100) = 1.39$, $p = 0.21$]. However, TauP301L mice made significantly more errors during acquisition [Tg main effect: $F(2, 25) = 4.32$, $p = 0.03$], regardless of day [Tg × Day interaction: $F(8, 100) = 1.64$, $p = 0.12$] (Fig. 3a). Examination of the 24-h probe trial in 30-s epochs, as previously reported (e.g., Devan *et al.* 2003), indicated that TauP301L mice made significantly more errors in the 30- to 60-s epoch [$F(2, 23) = 3.98$, $p = 0.03$)] (Fig. 3b). When the total errors in the 24-h probe were compared, TauP301L mice made marginally more errors across the entire 90-s probe trial [$F(2, 23) = 3.13, p = 0.06$)] (Fig. 3c). For the 1-week probe trial, there were no differences among the groups for total errors, errors in the three epochs, or latency ($ps > 0.05$; data not shown).

TauP301L mice exhibit hippocampal glutamate dysregulation

Tonic glutamate levels were not significantly different in the DG [$F(2, 17) = 0.15$; $p = 0.86$], CA3 [$F(2, 16) = 0.11$; $p = 0.89$], or CA1 [$F(2, 17) = 0.58$; $p = 0.57$] among the controls, TauWT, or TauP301L mice (Fig. 4a). To examine the capacity for glutamate release, KCl was delivered via a micropipette. Local application of 50–100 nL of 70 mM KCl produced reproducible glutamate release in all regions of the hippocampus. The amplitudes of KCL-evoked glutamate release in the CA1 [$F(2, 18) = 1.31$; $p = 0.29$] were similar

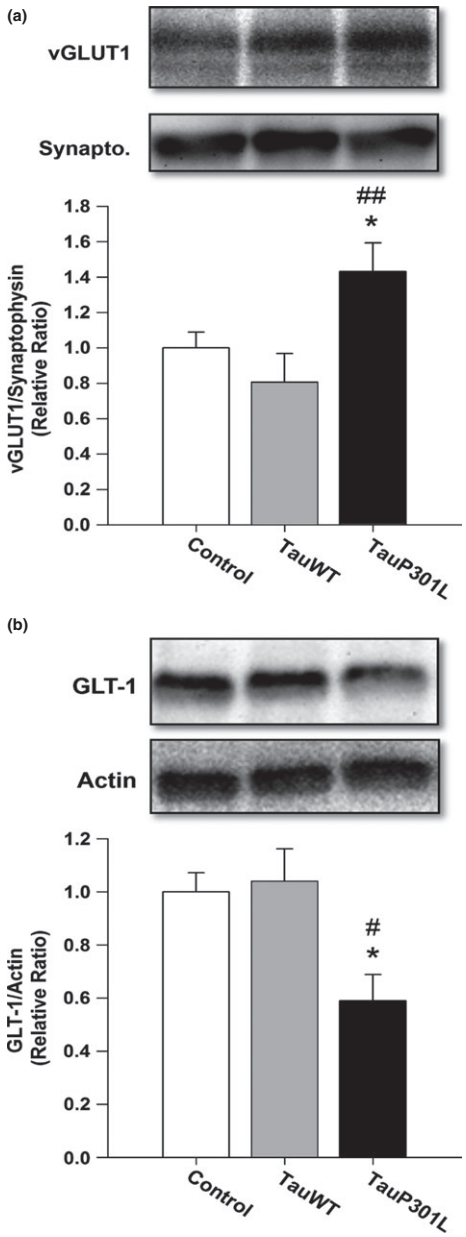

Fig. 2 TauP301L mice exhibit increased vesicular glutamate transporter (vGLUT1) expression and decreased glutamate transporter 1 (GLT-1) expression in the hippocampus. (a) vGLUT1 expression was significantly increased in hippocampal tissue of TauP301L mice. (b) In contrast, GLT-1 expression was significantly decreased in TauP301L mice (mean ± SEM; $*p < 0.05$ control vs. TauP301L, $\#p < 0.05$ TauWT vs. TauP301L, $\#\#p < 0.01$ TauWT vs. TauP301L, $n = 5$–6/group).

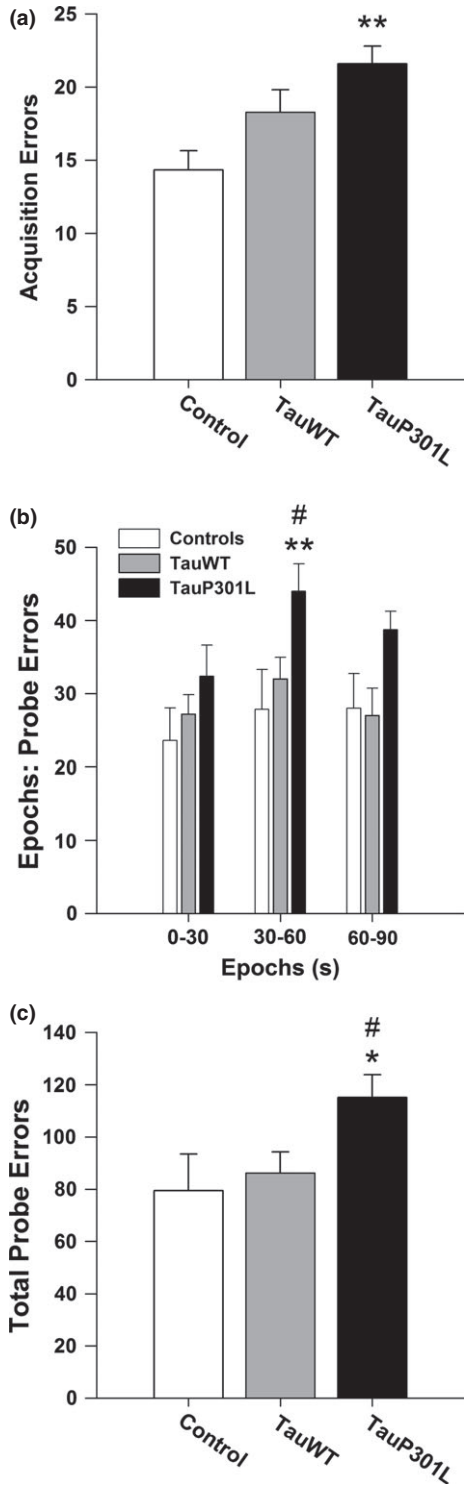

Fig. 3 TauP301L mice exhibit memory deficits in the Barnes maze (BM) task. (a) Errors during acquisition were significantly increased for TauP301L mice. (b) TauP301L mice made more errors during the 30- to 60-s epoch. (c) TauP301L mice exhibited marginally more errors during probe trials (mean ± SEM; $*p < 0.05$ control vs. TauP301L, $**p < 0.01$ control vs. TauP301L, $\#p < 0.05$ TauWT vs. TauP301L, $n = 7$–11/group; controls = 7, TauWT = 11, and TauP301L = 9).

among the groups, whereas in the DG [$F(2, 17) = 4.14$; $p = 0.03$] and CA3 [$F(2, 17) = 4.33$, $p = 0.03$], the amplitude of KCl-evoked glutamate release was four and seven times larger in TauP301L mice, respectively (Fig. 4b and c).

Rapid application of glutamate into the extracellular space allowed us to mimic endogenous glutamate release and examine glutamate clearance back to baseline *in vivo*. To ensure differences in net AUC among the groups following application of endogenous glutamate were due to alterations in clearance and not differences in amount of endogenous glutamate applied, we first compared the amplitude of glutamate signals following the administration of exogenous glutamate; no differences in amplitude were observed among controls, TauWT, and TauP301L mice in the DG [$F(2, 14) = 0.88$; $p = 0.44$], CA3 [$F(2, 12) = 0.47$; $p = 0.64$], and CA1 [$F(2, 14) = 0.04$; $p = 0.96$] (Fig. 5a), suggesting similar application of exogenous glutamate. We next examined Trise, the time for signal to reach maximum amplitude, to determine if transgene status altered diffusion of glutamate in the extracellular space; Trise was not significantly different among the groups DG [$F(2, 14) = 0.33$; $p = 0.72$], CA3 [$F(2, 12) = 0.19$; $p = 0.83$], and CA1 [$F(2, 14) = 0.58$; $p = 0.57$] (Fig. 5b), suggesting any reductions in glutamate clearance were not due to diffusion from the point source (micropipette) to the MEA (Sykova *et al.* 1998). Because neither amplitude nor Trise differed among the groups, any differences in net AUC likely result from decreases in glutamate uptake. Following exogenous application of glutamate, TauP301L mice exhibited an increased net AUC in the DG [$F(2, 14) = 5.21$, $p = 0.02$], CA3 [$F(2, 12) = 7.37$; $p = 0.008$], and CA1 [$F(2, 14) = 8.75$; $p = 0.003$] (Fig. 5c and d), suggesting reduced glutamate uptake in all three regions of the hippocampus.

Glutamate regulation correlates with Barnes maze performance

We next sought to determine whether errors in the BM correlated with glutamate regulation (Table 2). For KCl-evoked release, the amplitude of evoked glutamate release in the CA3 was significantly correlated with BM performance ($p = 0.002$), whereas for the DG and CA1 regions, there was no relation between KCl-evoked release and performance ($p = 0.21$ and $p = 0.21$, respectively). In contrast, for clearance of exogenous glutamate, the opposite pattern was observed. Errors in the BM were significantly correlated with clearance (net AUC) in the DG ($p = 0.0004$) and CA1 ($p = 0.002$) but not the CA3 ($p = 0.067$).

Pathological tau conformation and phosphorylation

A panel of antibodies (Table 1) directed at biochemical changes in tau associated with AD was used to determine the extent of tau pathology at the time of behavioral and glutamate testing. As previously reported (Andorfer *et al.*

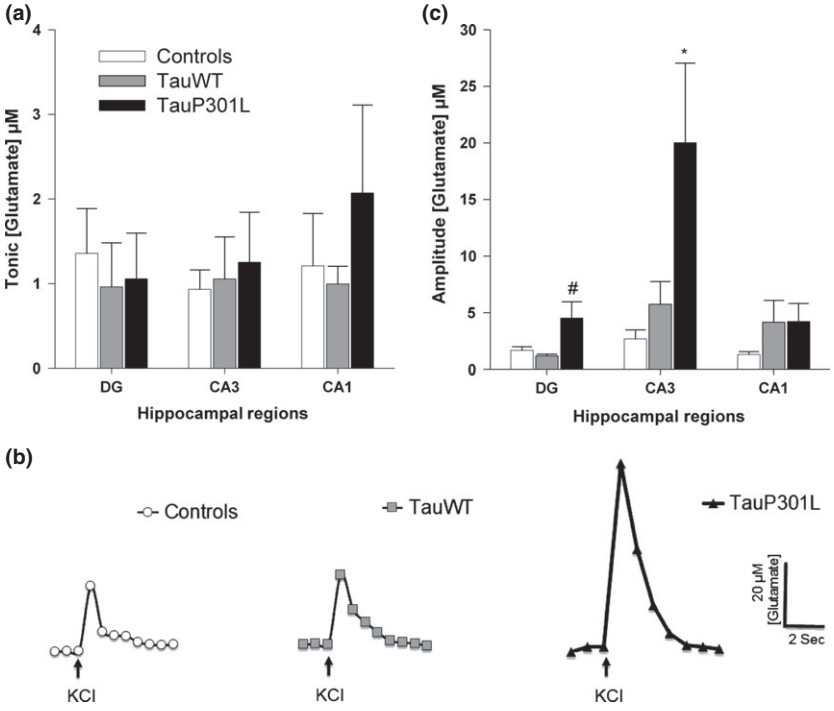

Fig. 4 Tonic and potassium chloride (KCl)-evoked release of glutamate in the dentate gyrus (DG), cornu ammonis (CA)3, and CA1 regions of the hippocampus. (a) Tonic glutamate levels were not significantly different in the hippocampus. (b) Baseline-matched representative recordings of KCl-evoked glutamate release in the CA3 showed that there was a significant increase in the amplitude of glutamate release in TauP301L mice. Local application of KCl (↑) produced a robust increase in extracellular glutamate that rapidly returned to tonic levels. (c) The average amplitudes of KCl-evoked glutamate release in the DG and CA3 regions of hippocampus were significantly increased in the TauP301L mice after the local application of 50–100 nL of 70 mM KCl (mean ± SEM; $*p < 0.05$ control vs. TauP301L; $\#p < 0.05$ TauWT vs. TauP301L; $n = 6$–7/group).

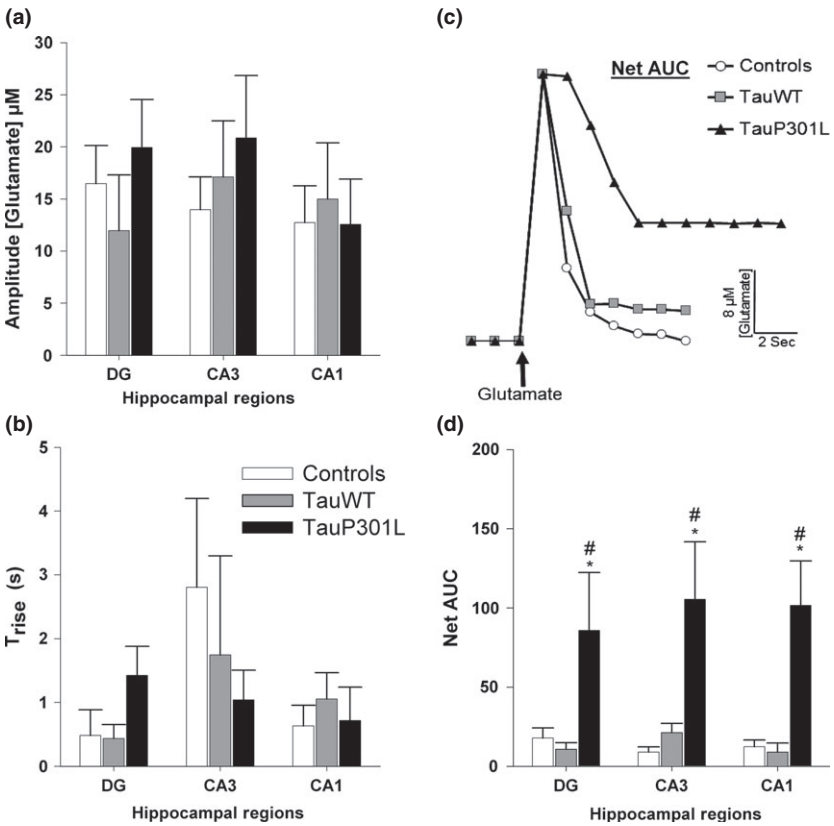

Fig. 5 Reduced glutamate clearance in TauP301L mice following exogenous glutamate application in the dentate gyrus (DG), cornu ammonis (CA)3, and CA1 regions of the hippocampus. (a) The amplitude of glutamate signal was similar among groups in each region. (b) Trise, an indicator of glutamate diffusion, was similar among the groups in each region. (c) Representative glutamate signals in the CA1 from local application of 200 µM glutamate (↑) in controls (circles), TauWT (squares), and TauP301L (triangles) mice. TauP301L mice showed significant decreases in net area under the curve (AUC). (d) The net AUC was increased in TauP301L mice in all three regions of the hippocampus in TauP301L mice, indicating reduced glutamate uptake (mean ± SEM; $*p < 0.05$ control vs. TauP301L, $\#p < 0.05$ TauWT vs. TauP301L; $n = 6$–7/group).

2003; Ramsden *et al.* 2005; Hunsberger *et al.* 2014), the earliest positive labeling in the hippocampus was identified using CP-13 and MC-1, which detect phosphorylation and conformation-specific changes, respectively (Fig. 6a and b). In contrast, when AT-8 and PG-5 were used to examine the presence of pre-tangles (accumulations of non-argyrophilic

Table 2 Correlations between glutamate dysregulation and errors in the Barnes maze (significant p-values in bold).

	DG	CA3	CA1
KCl-evoked release vs. errors	Errors = 16.83 + 0.58*Amp r (21)= 0.29, p = 0.21	Errors = 16.14 + 0.024*Amp r (20)= 0.64, **p = 0.002**	Errors = 17.04 + 0.38*Amp r (20) = 0.29, p = 0.21
Clearance vs. errors	Errors = 14.97 + 0.064*AUC r (19) = 0.76, **p = 0.0004**	Errors = 15.67 + 0.039*AUC r (18) = 0.48, p = 0.067	Errors = 15.07 + 0.053*AUC r (18) = 0.69, **p = 0.002**

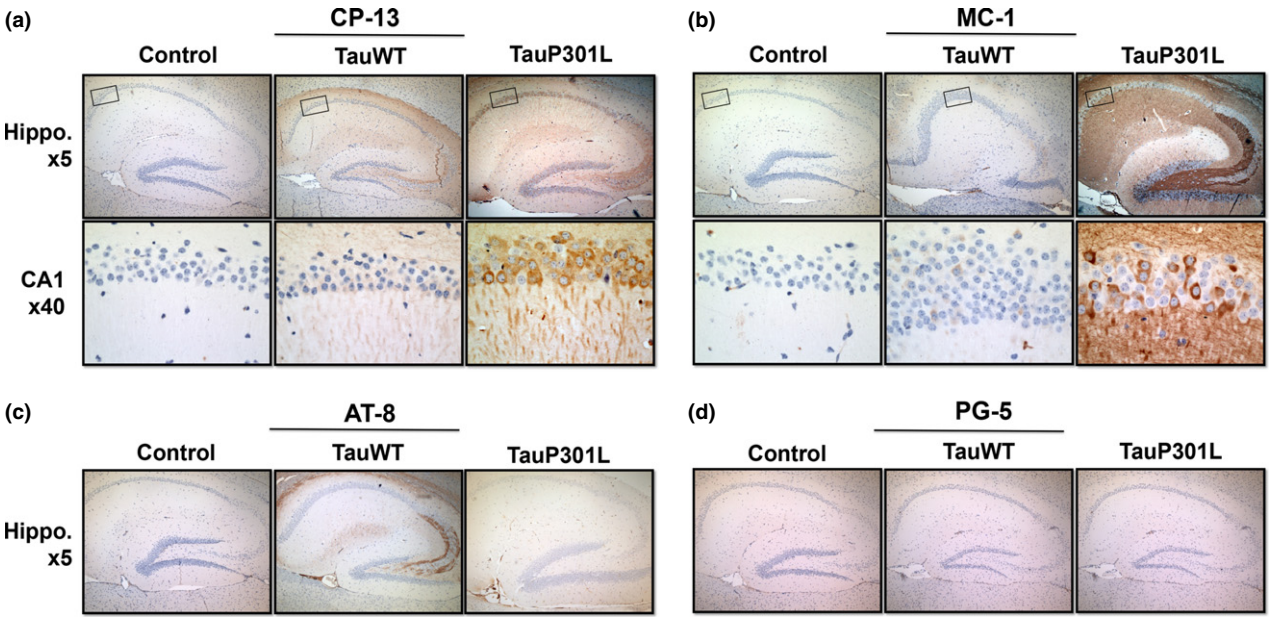

Fig. 6 Early tau pathology in TauP301L mice. (a) IHC studies revealed abnormal tau conformation and phosphorylation when using the early pathological markers of AD, CP-13, and MC-1. (b) No differences were observed when the pre-tangle marker AT-8 and PG-5 were examined. Conformational changes determined using: MC-1, amino acids 7–9 and amino acids 326–300, and phosphorylation changes detected using: CP-13, pSer^{202}; AT-8, pSer^{202}/pThr^{205}; PG-5, pSer^{409}. No positive labeling was observed after parallel processing of control tissue or TauWT mice (n = 4/group). Staining was consistent across all TauP301L mice (n = 4). Boxes indicate areas shown at higher magnification. Original magnifications: ×5 for hippocampus (Hippo.) and ×40 for cornu ammonis 1 (CA1).

hyperphosphorylated tau in the neuronal cell body) in the hippocampus, no positive staining was observed with either antibody (Fig. 6c and d). Similarly, no NFTs were observed after staining with Bielschowsky silver (data now shown). To determine if there was readily detectable neuron loss, hematoxylin and eosin (H&E)-stained tissue among the groups was compared. To further supplement the examination of neuronal loss, tissue was also incubated with a neuron-specific antibody (NeuN). After 3 months of tau expression, there was no readily detectable cell loss in the hippocampus of TauP301L mice using either H&E or NeuN (Fig. 7).

Discussion

We examined the extent of glutamate dysregulation in a TauP301L mouse model of AD known to exhibit electrophysiological hyperexcitability prior to tangle deposition or neuronal death (Crimins *et al.* 2012). This study is the first to use *in vivo* amperometry to examine glutamate dysregulation in the DG, CA3, and CA1 subregions of the hippocampus in an AD mouse model. The hippocampal-dependent BM task was used to relate pathological glutamate changes with functional deficits. Although tonic glutamate levels were unaltered in all three regions of the hippocampus, KCl-evoked glutamate release in the DG and CA3 was significantly increased in TauP301L mice, and glutamate clearance was significantly decreased in all three regions. This increase in release and decrease in clearance was associated with an increase in vGLUT1 and a decrease in GLT-1 expression, respectively.

The BM is a spatial memory task that requires animals to use spatial cues around the room to learn the position of a hole that can be used to escape the brightly lit, aversive, open surface of the maze. Rodents with hippocampal damage

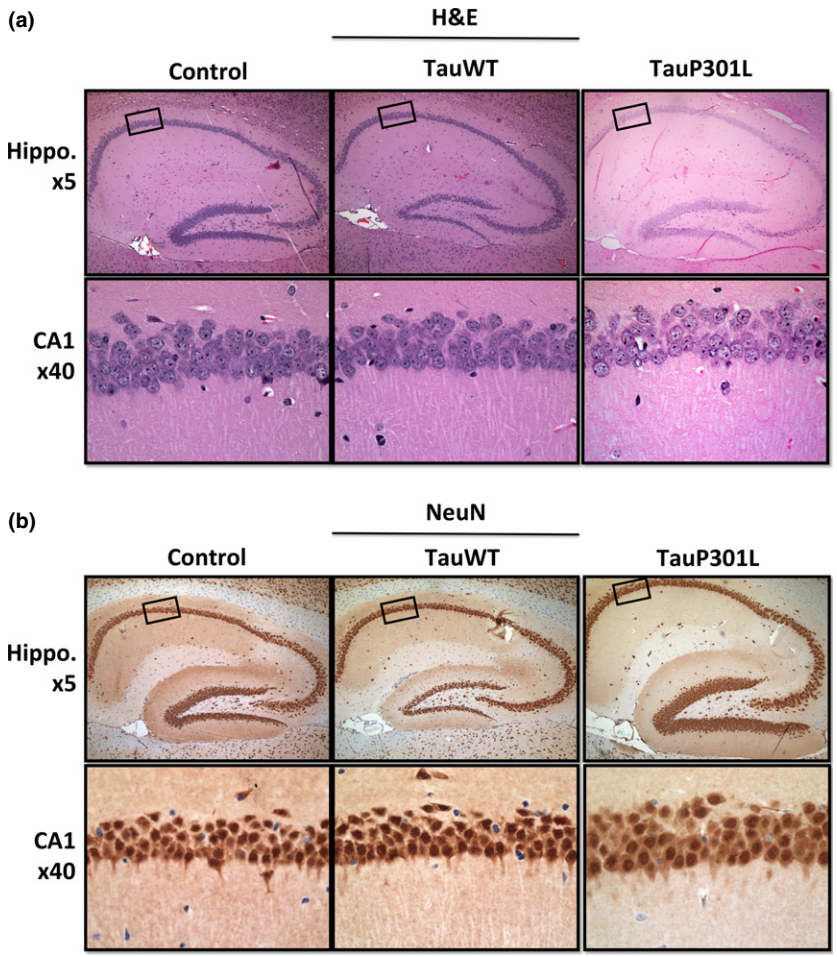

Fig. 7 No neuron loss was readily detectable in TauP301L mice. Neuron loss was not readily detectable when compared using (a) hematoxylin and eosin (H&E) or (b) neuron-specific antibody (NeuN). Boxes indicate area shown at higher magnification. Representative images shown and were consistent across all TauP301L mice ($n = 4$). Original magnifications: ×5 for hippocampus (Hippo.) and ×40 for CA1.

show impaired performance in the BM, suggesting that this is a hippocampal-dependent task (Fox *et al.* 1998; Pompl *et al.* 1999). Unlike the commonly used hippocampal-dependent Morris water maze, the BM task does not require the mice to swim and is therefore considered less anxiogenic (Harrison *et al.* 2009), a notion supported by findings of lower plasma corticosterone in rodents examined after the BM compared to the Morris water maze task (Harrison *et al.* 2009). Because stress is related to both an increase in extracellular glutamate (Popoli *et al.* 2012) and an increase in tau hyperphosphorylation (Sotiropoulos *et al.* 2011; Popoli *et al.* 2012), the BM task was identified as a more suitable measurement of memory for this study. The present findings confirm that the BM is a sensitive task for use with TauP301L mice, capable of detecting the subtle differences resulting from a short duration of P301L tau expression.

The tonic glutamate levels observed in this study (1–3 μM) were similar to the levels previously reported in the hippocampus of microdialysis studies using rats (1–4 μM) (Lerma *et al.* 1986; Miele *et al.* 1996; Herman and Jahr 2007). Interestingly, *in vitro* studies using hippocampal brain slices suggest much lower ambient glutamate concentrations, with values closer to 0.025 μM (Herman and Jahr 2007). The reason for these discrepancies between *in vitro* and *in vivo* studies remains unclear and warrants further investigation.

P301L tau expression did not alter tonic glutamate levels. The lack of differences in tonic glutamate for TauP301L mice is somewhat surprising given the increased vGLUT1 expression and KCl-evoked release observed in these mice. However, *in vitro* studies using hippocampal slices suggest that tonic glutamate levels are not dependent on, or altered by, vesicular glutamate release but may instead be due to differences in glia-dependent release of glutamate (Jabaudon *et al.* 1999; Cavelier and Attwell 2005; Le Meur *et al.* 2007). *In vivo* studies using MEAs provide indirect support for this idea. In mice with traumatic brain injury, striatal tonic levels were increased, yet KCl-evoked released remained unchanged (Hinzman *et al.* 2010). MEA research with aging rats shows that the opposite is also possible; aged rats exhibited increased KCl-evoked release, but unaltered levels of tonic glutamate (Stephens *et al.* 2011), similar to the present findings. Future studies are needed to further delineate and confirm glia as primary sources of tonic extracellular glutamate.

The exact mechanism by which P301L tau expression increases KCl-evoked glutamate release in the DG and CA3 is not known, but the increased VGLUT expression observed in TauP301L mice might explain the increase in glutamate release. The number of VGLUT molecules has a direct impact on the number of glutamate molecules released by a single synaptic vesicle during exocytosis (Wilson *et al.* 2005; Herzog *et al.* 2006), and over-expression of VGLUT results in increased glutamate release, leading to excitotoxic neurodegeneration and a shortened lifespan (Daniels *et al.* 2011). An important future direction is to determine whether the increase in vGLUT1 expression in TauP301L mice is limited to the DG and CA3 regions of the hippocampus and whether reducing vGLUT1 expression attenuates the increased release observed in TauP301L mice.

In many neurodegenerative diseases, including amyotrophic lateral sclerosis (Rothstein *et al.* 1995), Huntington's disease (Arzberger *et al.* 1997), Parkinson's disease (Ferrarese *et al.* 1999), and AD (Masliah *et al.* 2000), astrocytic glutamate transporter (GLT) expression is decreased. However, because brains are often examined at the end-stage of these diseases, neuronal loss is often extensive, making it difficult to discern the role of GLTs in the pathogenesis of these diseases. To better examine the role of GLTs in the etiology of AD, mouse models have been examined. In JNPL-c tau transgenic mice, which also express the P301L mutation in tau, glutamate transporter (GLT-1) expression was increased by about 25% and was associated with improved stroke outcome (Liao *et al.* 2009). Surprisingly, we observed exactly the opposite effect of P301L tau expression: a decrease in GLT-1 expression. There are a few differences between the two studies that may account for this discrepancy. First, the previous finding of increased GLT-1 expression was observed after only 2 months of tau expression (Liao *et al.* 2009), whereas mice in this study expressed tau for longer. Previous work with another P301L model suggests 2 months of P301L tau expression, before hyperphosphorylation such as that observed in this study is present, results in increased long-term potentiation and improved cognitive performance (Boekhoorn *et al.* 2006). Because Liao and colleagues did not examine memory, it remains unclear whether the increased GLT-1 expression was associated with improved cognitive performance. It is possible GLT-1 expression increases and then decreases with longer durations of tau expression. A second difference involves the age of onset of P301L tau expression. Mice in the previous study expressed tau during development (Liao *et al.* 2009), and thus, it is possible that the increase in GLT-1 resulted from developmental tau expression. Previously published work suggests that developmental P301L tau expression produces alterations not observed following adult-onset tau expression (Caouette *et al.* 2013). Such a finding is not surprising given the importance of tau in brain development (Wang and Liu 2008). Examination of GLT-1 at earlier and later time points in the adult-onset P301L model would help address these issues.

One potential caveat of this study concerns the high spatial resolution of the microelectrodes (Burmeister *et al.* 2000, 2002). Because of the high spatial resolution, it is possible that different coordinates within the various subregions of the hippocampus would result in different effects than those observed here. In fact, when examined using MEAs, tonic glutamate levels were increased in rats with traumatic brain injury but only at certain depths within the striatum (Hinzman *et al.* 2010); increases in tonic glutamate levels were observed at a depth of 4.0 mm, but not at 4.5 mm or 5.0 mm. Thus, examination of TauP301L mice using slightly different coordinates might reveal different results. Although the spatial resolution can be a limitation, it is also a benefit, allowing subregional analyses and measurements of fast transmission close to the synapse.

In conclusion, we used MEAs in combination with the TauP301L mouse model to examine the effects of P301L tau expression on glutamate signaling, without other mediators, such as Aβ plaques, tangles, and neuronal loss. Our results demonstrate that memory-impaired TauP301L mice exhibit an increase in KCL-evoked glutamate release in the DG and CA3 regions of the hippocampus and a decrease in glutamate clearance in the DG, CA3, and CA1 regions of the hippocampus. More research is needed to determine the specific mechanisms by which tau pathology alters glutamate regulation.

Acknowledgments and conflict of interest disclosure

This work was supported by the National Institute of General Medical Sciences (Reed - U54GM104942), the Alzheimer's Association (Reed - NIRG-12-242187), a WVU Faculty Research Senate Grant, and a WVU PSCOR grant. The content is solely the responsibility of the authors and does not necessarily represent the official views of the NIH or Alzheimer's Association. GG is the sole proprietor of Quanteon, LLC that makes the Fast-16 recording system used for glutamate measurements in this study.

All experiments were conducted in compliance with the ARRIVE guidelines.

References

Andorfer C., Kress Y., Espinoza M., de Silva R., Tucker K. L., Barde Y. A., Duff K. and Davies P. (2003) Hyperphosphorylation and aggregation of tau in mice expressing normal human tau isoforms. *J. Neurochem.* **86**, 582–590.

Arzberger T., Krampfl K., Leimgruber S. and Weindl A. (1997) Changes of NMDA receptor subunit (NR1, NR2B) and glutamate transporter (GLT1) mRNA expression in Huntington's disease–an in situ hybridization study. *J. Neuropathol. Exp. Neurol.* **56**, 440–454.

Auld D. S., Kornecook T. J., Bastianetto S. and Quirion R. (2002) Alzheimer's disease and the basal forebrain cholinergic system:

relations to beta-amyloid peptides, cognition, and treatment strategies. *Prog. Neurobiol.* **68**, 209–245.

Bakker A., Krauss G. L., Albert M. S. *et al.* (2012) Reduction of hippocampal hyperactivity improves cognition in amnestic mild cognitive impairment. *Neuron* **74**, 467–474.

Boekhoorn K., Terwel D., Biemans B. *et al.* (2006) Improved long-term potentiation and memory in young tau-P301L transgenic mice before onset of hyperphosphorylation and tauopathy. *J. Neurosci.* **26**, 3514–3523.

Bondi M. W., Houston W. S., Eyler L. T. and Brown G. G. (2005) fMRI evidence of compensatory mechanisms in older adults at genetic risk for Alzheimer disease. *Neurology* **64**, 501–508.

Bookheimer S. Y., Strojwas M. H., Cohen M. S., Saunders A. M., Pericak-Vance M. A., Mazziotta J. C. and Small G. W. (2000) Patterns of brain activation in people at risk for Alzheimer's disease. *N. Engl. J. Med.* **343**, 450–456.

Buckner R. L., Snyder A. Z., Shannon B. J. *et al.* (2005) Molecular, structural, and functional characterization of Alzheimer's disease: evidence for a relationship between default activity, amyloid, and memory. *J. Neurosci.* **25**, 7709–7717.

Burmeister J. J. and Gerhardt G. A. (2001) Self-referencing ceramic-based multisite microelectrodes for the detection and elimination of interferences from the measurement of L-glutamate and other analytes. *Anal. Chem.* **73**, 1037–1042.

Burmeister J. J., Moxon K. and Gerhardt G. A. (2000) Ceramic-based multisite microelectrodes for electrochemical recordings. *Anal. Chem.* **72**, 187–192.

Burmeister J. J., Pomerleau F., Palmer M., Day B. K., Huettl P. and Gerhardt G. A. (2002) Improved ceramic-based multisite microelectrode for rapid measurements of L-glutamate in the CNS. *J. Neurosci. Methods* **119**, 163–171.

de Calignon A., Polydoro M., Suarez-Calvet M. *et al.* (2012) Propagation of tau pathology in a model of early Alzheimer's disease. *Neuron* **73**, 685–697.

Caouette D., Xie Z., Milici A., Kuhn M., Bocan T. and Yang D. (2013) Perinatal suppression of Tau P301L has a long lasting preventive effect against neurodegeneration. *Int. J. Neuropathol.* **1**, 53–69.

Cavelier P. and Attwell D. (2005) Tonic release of glutamate by a DIDS-sensitive mechanism in rat hippocampal slices. *J. Physiol.* **564**, 397–410.

Celone K. A., Calhoun V. D., Dickerson B. C. *et al.* (2006) Alterations in memory networks in mild cognitive impairment and Alzheimer's disease: an independent component analysis. *J. Neurosci.* **26**, 10222–10231.

Crimins J. L., Rocher A. B. and Luebke J. I. (2012) Electrophysiological changes precede morphological changes to frontal cortical pyramidal neurons in the rTg4510 mouse model of progressive tauopathy. *Acta Neuropathol.* **124**, 777–795.

Daniels R. W., Miller B. R. and DiAntonio A. (2011) Increased vesicular glutamate transporter expression causes excitotoxic neurodegeneration. *Neurobiol. Dis.* **41**, 415–420.

Day B. K., Pomerleau F., Burmeister J. J., Huettl P. and Gerhardt G. A. (2006) Microelectrode array studies of basal and potassium-evoked release of L-glutamate in the anesthetized rat brain. *J. Neurochem.* **96**, 1626–1635. Epub 2006 Jan 1625.

Dennis N. A., Browndyke J. N., Stokes J., Need A., Burke J. R., Welsh-Bohmer K. A. and Cabeza R. (2010) Temporal lobe functional activity and connectivity in young adult APOE varepsilon4 carriers. *Alzheimers Dement.* **6**, 303–311.

Devan B. D., Stouffer E. M., Petri H. L., McDonald R. J. and Olds J. L. (2003) Partial reinforcement across trials impairs escape performance but spares place learning in the water maze. *Behav. Brain Res.* **141**, 91–104.

Dickerson B. C., Salat D. H., Bates J. F. *et al.* (2004) Medial temporal lobe function and structure in mild cognitive impairment. *Ann. Neurol.* **56**, 27–35.

Dickerson B. C., Salat D. H., Greve D. N. *et al.* (2005) Increased hippocampal activation in mild cognitive impairment compared to normal aging and AD. *Neurology* **65**, 404–411.

Ferrarese C., Zoia C., Pecora N. *et al.* (1999) Reduced platelet glutamate uptake in Parkinson's disease. *J. Neural Transm.* **106**, 685–692.

Filippini N., MacIntosh B. J., Hough M. G., Goodwin G. M., Frisoni G. B., Smith S. M., Matthews P. M., Beckmann C. F. and Mackay C. E. (2009) Distinct patterns of brain activity in young carriers of the APOE-epsilon4 allele. *Proc. Natl Acad. Sci. USA* **106**, 7209–7214.

Fox G. B., Fan L., LeVasseur R. A. and Faden A. I. (1998) Effect of traumatic brain injury on mouse spatial and nonspatial learning in the Barnes circular maze. *J. Neurotrauma* **15**, 1037–1046.

Friedemann M. N. and Gerhardt G. A. (1992) Regional effects of aging on dopaminergic function in the Fischer-344 rat. *Neurobiol. Aging* **13**, 325–332.

Grady C. L., McIntosh A. R., Beig S., Keightley M. L., Burian H. and Black S. E. (2003) Evidence from functional neuroimaging of a compensatory prefrontal network in Alzheimer's disease. *J. Neurosci.* **23**, 986–993.

Hamalainen A., Pihlajamaki M., Tanila H., Hanninen T., Niskanen E., Tervo S., Karjalainen P. A., Vanninen R. L. and Soininen H. (2007) Increased fMRI responses during encoding in mild cognitive impairment. *Neurobiol. Aging* **28**, 1889–1903.

Harrison F. E., Hosseini A. H. and McDonald M. P. (2009) Endogenous anxiety and stress responses in water maze and Barnes maze spatial memory tasks. *Behav. Brain Res.* **198**, 247–251.

Hascup E. R., af Bjerken S., Hascup K. N., Pomerleau F., Huettl P., Stromberg I. and Gerhardt G. A. (2009) Histological studies of the effects of chronic implantation of ceramic-based microelectrode arrays and microdialysis probes in rat prefrontal cortex. *Brain Res.* **1291**, 12–20.

Herman M. A. and Jahr C. E. (2007) Extracellular glutamate concentration in hippocampal slice. *J. Neurosci.* **27**, 9736–9741.

Herzog E., Takamori S., Jahn R., Brose N. and Wojcik S. M. (2006) Synaptic and vesicular co-localization of the glutamate transporters VGLUT1 and VGLUT2 in the mouse hippocampus. *J. Neurochem.* **99**, 1011–1018.

Hinzman J. M., Thomas T. C., Burmeister J. J., Quintero J. E., Huettl P., Pomerleau F., Gerhardt G. A. and Lifshitz J. (2010) Diffuse brain injury elevates tonic glutamate levels and potassium-evoked glutamate release in discrete brain regions at two days post-injury: an enzyme-based microelectrode array study. *J. Neurotrauma* **27**, 889–899.

Hinzman J. M., Thomas T. C., Quintero J. E., Gerhardt G. A. and Lifshitz J. (2012) Disruptions in the regulation of extracellular glutamate by neurons and glia in the rat striatum two days after diffuse brain injury. *J. Neurotrauma* **29**, 1197–1208.

Hölscher C. (1999) Stress impairs performance in spatial water maze learning tasks. *Behav. Brain Res.* **100**, 225–235.

Hoover B. R., Reed M. N., Su J. *et al.* (2010) Tau mislocalization to dendritic spines mediates synaptic dysfunction independently of neurodegeneration. *Neuron* **68**, 1067–1081.

Hunsberger H. C., Rudy C. C., Weitzner D. S., Zhang C., Tosto D. E., Knowlan K., Xu Y. and Reed M. N. (2014) Effect size of memory deficits in mice with adult-onset P301L tau expression. *Behav. Brain Res.* **272**, 181–195.

Jabaudon D., Shimamoto K., Yasuda-Kamatani Y., Scanziani M., Gahwiler B. H. and Gerber U. (1999) Inhibition of uptake unmasks

rapid extracellular turnover of glutamate of nonvesicular origin. *Proc. Natl Acad. Sci. USA* **96**, 8733–8738.

Koh M. T., Haberman R. P., Foti S., McCown T. J. and Gallagher M. (2010) Treatment strategies targeting excess hippocampal activity benefit aged rats with cognitive impairment. *Neuropsychopharmacology* **35**, 1016–1025.

Le Meur K., Galante M., Angulo M. C. and Audinat E. (2007) Tonic activation of NMDA receptors by ambient glutamate of non-synaptic origin in the rat hippocampus. *J. Physiol.* **580**, 373–383.

Lerma J., Herranz A. S., Herreras O., Abraira V. and Martin del Rio R. (1986) In vivo determination of extracellular concentration of amino acids in the rat hippocampus. A method based on brain dialysis and computerized analysis. *Brain Res.* **384**, 145–155.

Liao G., Zhou M., Cheung S., Galeano J., Nguyen N., Baudry M. and Bi X. (2009) Reduced early hypoxic/ischemic brain damage is associated with increased GLT-1 levels in mice expressing mutant (P301L) human tau. *Brain Res.* **1247**, 159–170.

Liu B., Wang S., Brenner M., Paton J. F. and Kasparov S. (2008) Enhancement of cell-specific transgene expression from a Tet-Off regulatory system using a transcriptional amplification strategy in the rat brain. *J. Gene Med.* **10**, 583–592.

Liu L., Drouet V., Wu J. W., Witter M. P., Small S. A., Clelland C. and Duff K. (2012) Trans-synaptic spread of tau pathology in vivo. *PLoS ONE* **7**, e31302.

Masliah E., Alford M., Mallory M., Rockenstein E., Moechars D. and Van Leuven F. (2000) Abnormal glutamate transport function in mutant amyloid precursor protein transgenic mice. *Exp. Neurol.* **163**, 381–387.

Mattinson C. E., Burmeister J. J., Quintero J. E., Pomerleau F., Huettl P. and Gerhardt G. A. (2011) Tonic and phasic release of glutamate and acetylcholine neurotransmission in sub-regions of the rat prefrontal cortex using enzyme-based microelectrode arrays. *J. Neurosci. Methods* **202**, 199–208.

Mayford M., Bach M. E., Huang Y. Y., Wang L., Hawkins R. D. and Kandel E. R. (1996) Control of memory formation through regulated expression of a CaMKII transgene. *Science* **274**, 1678–1683.

McAfoose J., Koerner H. and Baune B. T. (2009) The effects of TNF deficiency on age-related cognitive performance. *Psychoneuroendocrinology* **34**, 615–619.

McLay R. N., Freeman S. M. and Zadina J. E. (1998) Chronic corticosterone impairs memory performance in the Barnes maze. *Physiol. Behav.* **63**, 933–937.

Miele M., Berners M., Boutelle M. G., Kusakabe H. and Fillenz M. (1996) The determination of the extracellular concentration of brain glutamate using quantitative microdialysis. *Brain Res.* **707**, 131–133.

Miller S. L., Fenstermacher E., Bates J., Blacker D., Sperling R. A. and Dickerson B. C. (2008) Hippocampal activation in adults with mild cognitive impairment predicts subsequent cognitive decline. *J. Neurol. Neurosurg. Psychiatry* **79**, 630–635.

Nath S., Agholme L., Kurudenkandy F. R., Granseth B., Marcusson J. and Hallbeck M. (2012) Spreading of neurodegenerative pathology via neuron-to-neuron transmission of beta-amyloid. *J. Neurosci.* **32**, 8767–8777.

Nickell J., Salvatore M. F., Pomerleau F., Apparsundaram S. and Gerhardt G. A. (2007) Reduced plasma membrane surface expression of GLAST mediates decreased glutamate regulation in the aged striatum. *Neurobiol. Aging* **28**, 1737–1748.

Nimchinsky E. A., Yasuda R., Oertner T. G. and Svoboda K. (2004) The number of glutamate receptors opened by synaptic stimulation in single hippocampal spines. *J. Neurosci.* **24**, 2054–2064.

Palop J. J., Chin J. and Mucke L. (2006) A network dysfunction perspective on neurodegenerative diseases. *Nature* **443**, 768–773.

Paxinos G. and Franklin K. (2012) Mouse Brain in Stereotaxic Coordinates. Academic Press, Waltham Massachusetts.

Pettit D. L. and Augustine G. J. (2000) Distribution of functional glutamate and GABA receptors on hippocampal pyramidal cells and interneurons. *J. Neurophysiol.* **84**, 28–38.

Planel E., Miyasaka T., Launey T. *et al.* (2004) Alterations in glucose metabolism induce hypothermia leading to tau hyperphosphorylation through differential inhibition of kinase and phosphatase activities: implications for Alzheimer's disease. *J. Neurosci.* **24**, 2401–2411.

Pompl P. N., Mullan M. J., Bjugstad K. and Arendash G. W. (1999) Adaptation of the circular platform spatial memory task for mice: use in detecting cognitive impairment in the APP(SW) transgenic mouse model for Alzheimer's disease. *J. Neurosci. Methods* **87**, 87–95.

Popoli M., Yan Z., McEwen B. S. and Sanacora G. (2012) The stressed synapse: the impact of stress and glucocorticoids on glutamate transmission. *Nat. Rev. Neurosci.* **13**, 22–37.

Quiroz Y. T., Budson A. E., Celone K., Ruiz A., Newmark R., Castrillon G., Lopera F. and Stern C. E. (2010) Hippocampal hyperactivation in presymptomatic familial Alzheimer's disease. *Ann. Neurol.* **68**, 865–875.

Ramsden M., Kotilinek L., Forster C. *et al.* (2005) Age-dependent neurofibrillary tangle formation, neuron loss, and memory impairment in a mouse model of human tauopathy (P301L). *J. Neurosci.* **25**, 10637–10647.

Roberson E. D., Scearce-Levie K., Palop J. J., Yan F., Cheng I. H., Wu T., Gerstein H., Yu G. Q. and Mucke L. (2007) Reducing endogenous tau ameliorates amyloid beta-induced deficits in an Alzheimer's disease mouse model. *Science* **316**, 750–754.

Roberson E. D., Halabisky B., Yoo J. W. *et al.* (2011) Amyloid-beta/Fyn-induced synaptic, network, and cognitive impairments depend on tau levels in multiple mouse models of Alzheimer's disease. *J. Neurosci.* **31**, 700–711.

Rothstein J. D., Van Kammen M., Levey A. I., Martin L. J. and Kuncl R. W. (1995) Selective loss of glial glutamate transporter GLT-1 in amyotrophic lateral sclerosis. *Ann. Neurol.* **38**, 73–84.

Sanchez M. P., Gonzalo I., Avila J. and De Yebenes J. G. (2002) Progressive supranuclear palsy and tau hyperphosphorylation in a patient with a C212Y parkin mutation. *J. Alzheimers Dis.* **4**, 399–404.

Sanchez P. E., Zhu L., Verret L. *et al.* (2012) Levetiracetam suppresses neuronal network dysfunction and reverses synaptic and cognitive deficits in an Alzheimer's disease model. *Proc. Natl Acad. Sci. USA* **109**, E2895–E2903.

SantaCruz K., Lewis J., Spires T. *et al.* (2005) Tau suppression in a neurodegenerative mouse model improves memory function. *Science* **309**, 476–481.

Seeley W. W., Crawford R. K., Zhou J., Miller B. L. and Greicius M. D. (2009) Neurodegenerative diseases target large-scale human brain networks. *Neuron* **62**, 42–52.

Serrano-Pozo A., Frosch M. P., Masliah E. and Hyman B. T. (2011) Neuropathological alterations in Alzheimer disease. *Cold Spring Harb. Perspect Med.* **1**, a006189.

Sotiropoulos I., Catania C., Pinto L. G., Silva R., Pollerberg G. E., Takashima A., Sousa N. and Almeida O. F. (2011) Stress acts cumulatively to precipitate Alzheimer's disease-like tau pathology and cognitive deficits. *J. Neurosci.* **31**, 7840–7847.

Sperling R. (2007) Functional MRI studies of associative encoding in normal aging, mild cognitive impairment, and Alzheimer's disease. *Ann. N. Y. Acad. Sci.* **1097**, 146–155.

Stephens M. L., Quintero J. E., Pomerleau F., Huettl P. and Gerhardt G. A. (2011) Age-related changes in glutamate release in the CA3 and dentate gyrus of the rat hippocampus. *Neurobiol. Aging* **32**, 811–820.

Sykova E., Mazel T. and Simonova Z. (1998) Diffusion constraints and neuron-glia interaction during aging. *Exp. Gerontol.* **33**, 837–851.

Tan W., Cao X., Wang J., Lv H., Wu B. and Ma H. (2010) Tau hyperphosphorylation is associated with memory impairment after exposure to 1.5% isoflurane without temperature maintenance in rats. *Eur. J. Anaesthesiol.* **27**, 835–841.

Thies W. and Bleiler L. (2013) 2013 Alzheimer's disease facts and figures. *Alzheimers Dement.* **9**, 208–245.

Timmer N. M., Metaxas A., van der Stelt I., Kluijtmans L. A., van Berckel B. N. and Verbeek M. M. (2014) Cerebral level of vGlut1 is increased and level of glycine is decreased in TgSwDI mice. *J. Alzheimers Dis.* **39**, 89–101.

Trivedi M. A., Schmitz T. W., Ries M. L. *et al.* (2008) fMRI activation during episodic encoding and metacognitive appraisal across the lifespan: risk factors for Alzheimer's disease. *Neuropsychologia* **46**, 1667–1678.

Vossel K. A., Beagle A. J., Rabinovici G. D. *et al.* (2013) Seizures and epileptiform activity in the early stages of Alzheimer disease. *JAMA Neurol.* **70**, 1158–1166.

Wang J. Z. and Liu F. (2008) Microtubule-associated protein tau in development, degeneration and protection of neurons. *Prog. Neurobiol.* **85**, 148–175. Epub 2008 Mar 2022.

Ward N. S. and Frackowiak R. S. (2003) Age-related changes in the neural correlates of motor performance. *Brain* **126**, 873–888.

Wilson N. R., Kang J., Hueske E. V., Leung T., Varoqui H., Murnick J. G., Erickson J. D. and Liu G. (2005) Presynaptic regulation of quantal size by the vesicular glutamate transporter VGLUT1. *J. Neurosci.* **25**, 6221–6234.